

# Crystal structure, magnetism, and bonding of the hexagonal compounds $\text{Pd}_{1.63}\text{Mn}_{0.37}\text{Si}$ and $\text{Pd}_{1.82}\text{Mn}_{0.18}\text{Ge}$ related to the $\text{Fe}_2\text{P}$ structure

Srinivasa Thimmaiah<sup>†</sup>, Claudia Felser<sup>‡</sup>, and Ram Seshadri<sup>†</sup>

<sup>†</sup>Materials Department and Materials Research Laboratory  
University of California, Santa Barbara CA 93106  
seshadri@mrl.ucsb.edu

<sup>‡</sup>Institut für Anorganische Chemie und Analytische Chemie  
Johannes Gutenberg-Universität, Staudinger Weg 9, 55099 Mainz  
felser@uni-mainz.de

**Abstract.** We have used single crystal X-ray diffraction methods to establish the crystal structures of a compound in the Pd-Mn-Si system and in the Pd-Mn-Ge system. The title compounds have structures related to the  $\text{Fe}_2\text{P}$  structure type and are ferromagnetic with Curie temperatures above the room temperature. Density functional electronic structure calculations help to understand the nature of the local moment ferromagnetism in these compounds. However neither the electronic structure calculations nor the magnetic measurements provide any evidence of half-metallic behavior.

PACS numbers: 75.50.-y, 71.20.-b, 75.50.Cc

## 1. Introduction

In 1983, deGroot and coworkers[1] suggested that the electronic structure of the ferromagnetic half-Heusler compound NiMnSb possessed a curious characteristic; at the Fermi level, only states from one spin channel were populated; the other spin channel was gapped. They called such compounds half-metallic ferromagnets. The half metallic nature of NiMnSb has found experimental support from nulk measurement techniques such as positron annihilation.[2, 3] However, surface-sensitive techniques such as photoemission spectroscopy detect highly reduced spin polarization.[4, 5] The phenomena of half-metallicity has been identified as possessing a history that pre-dates NiMnSb – for example in certain pyrite compounds[6] and in certain chromium chalcospinels[7], as well as in the famous mixed-valent rare-earth manganites.[8]

Half-metallic ferromagnets are an important materials component in the emerging domain of spin-based electronics,[9, 10] and magnetic intermetallics deriving from Heusler and half-Heusler crystal structures have been the focus of much recent attention. Both the half-Heusler[11–14] and Heusler[15, 16] compounds obey certain simple electron counting rules that allow their saturation magnetic moments to be estimated from the number of valence electrons. One feature that emerges, particularly for the XYZ half-Heuslers[11, 14] is that covalency effects in parts of the structural network, specifically the YZ zinc blende lattice, play a crucial role in maintaining the half-metallic gap across a wide range of valence electron counts.

It is of interest to explore other equiatomic magnetic compounds with the general formula XYZ that are compositionally related to the half-Heusler structure but crystallize in other structures. For example, Johnson and Jeitschko explored a number of silicides and germanides[17] in the series Mn-Pd-Si and Mn-Pd-Ge. Bazela[18] has studied the magnetic properties of some related silicides and germanides without establishing the precise composition, assuming that the compounds were single phase. Vernière *et al.*[19] have reported the structure and magnetic properties of PdMnGe by neutron diffraction experiments. Eriksson *et al.*[20] have described a cubic compound with the formula  $Mn_8Pd_{15}Si_7$  in a filled  $Mg_6Cu_{16}Si_7$  structure type with complex magnetic behavior, including non-collinear spin ordering.

We thought it of interest to reexamine compounds in these systems in order to determine whether the hexagonal compounds are proximal to half-metallic ferromagnetism. Here we report on two compounds which occur as single crystals with  $Fe_2P$ -derived structures in the Pd-Mn-Si and Pd-Mn-Ge phase diagrams. We have reproduced polycrystalline samples with the compositions established by the single crystal structural studies. This has allowed magnetic studies on these compounds. In addition, we have performed density functional calculations on a typical compound from the Pd-Mn-Si system to better understand the nature of the magnetism.

## 2. Experimental details and crystal structure studies

Pd-Mn-X (X: Si and Ge) compounds were prepared from high purity metals by arc melting in an Ar atmosphere. A composition of 3:1:2 (Pd:Mn:X) was chosen for the preparation. The products obtained from arc melting were sealed in evacuated vitreous silica tubes and subsequently annealed first at 950°C for two days and then at 800°C for 5 to 10 days in order to improve the site ordering of the phases. Crystals were picked from crushed products and subject to single crystal diffraction studies. The phase purity of powder samples were checked using a Phillips (XPRT MPD, 45 kV 40 mA, Cu-K $\alpha$  radiation) powder diffractometer, followed by Rietveld refinement of the diffraction profiles. SQUID magnetization measurements were carried out in the temperature range 5 to 400 K using a Quantum Design MPMS 5XL SQUID magnetometer. Zero field cooled (ZFC) and field cooled (FC) magnetization as a function of temperature was at a constant field strength of 1000 Oe. In addition, isothermal  $M - H$  traces were recorded at different temperatures.

A small crystal of size  $0.12 \times 0.07 \times 0.06 \text{ mm}^3$  was picked from the Pd-Mn-Si sample from a sample that also contained MnSi as a minority phase. X-ray diffraction intensities were collected on Bruker CCD diffractometer (MoK $\alpha$  radiation,  $\lambda = 0.71073 \text{ \AA}$ ) at room temperature. The measured intensities were corrected for Lorentz and polarization effects and were further corrected for absorption using the SADABS program.[21] The structure solution was obtained using the SHELXS-97 program and refined using the SHELXL-97 as implemented in SHELXTL package using full-matrix least-squares refinement.[22] The structure was solved in the space group  $P\bar{6}2m$  (No. 189). The final refinement cycles used anisotropic displacement parameter and gave  $R_1 = 0.0264$  for 130 unique reflections. There was no evidence for strong correlation between refined parameters and thermal displacement parameters behaved normally. The suggested sample composition was Pd<sub>1.63</sub>Mn<sub>0.37</sub>Si.

The crystals from the Pd-Mn-Ge system were isolated from the sample consisting of Pd<sub>3</sub>MnGe<sub>2</sub> as a second phase (orthorhombic,  $Pnma$ ,  $a = 6.910(1) \text{ \AA}$ ,  $b = 3.146(1) \text{ \AA}$ ,  $c = 16.504(4) \text{ \AA}$ .[19, 23]) The majority of the sample consisted of the orthorhombic phase. Several attempts were made to isolate good quality crystals of the orthorhombic phase to confirm the structure independently but these were unsuccessful. However, good quality crystals were found to have hexagonal symmetry. A crystal of size  $0.10 \times 0.075 \times 0.06 \text{ mm}^3$  was selected for single crystal diffraction studies. The same procedures used previously were employed to obtain the crystal structure. The final refinement performed on  $F^2$  with 134 unique reflections gave  $R_1 = 0.0314$ . The suggested sample composition was Pd<sub>1.82</sub>Mn<sub>0.18</sub>Ge.

## 3. Computational studies

An ordered supercell was derived from the structure of Pd<sub>1.63</sub>Mn<sub>0.37</sub>Si with the composition Pd<sub>9</sub>Mn<sub>3</sub>Si<sub>6</sub>, and with an orthohexagonal unit cell in the space group  $Pmm2$

**Table 1.** Crystal structures of the Pd-Mn-Si and Pd-Mn-Ge compounds. Space group  $P\bar{6}2m$  (No. 189) obtained from single-crystal X-ray diffraction.

Pd-Mn-Si, $a = 6.5033(8) \text{ \AA}$ , $c = 3.4622(8) \text{ \AA}$ , $R = 2.6\%$						
Atom	Wyckoff Symbol	$x$	$y$	$z$	occupancy	$U_{eq.}(\text{\AA}^2)$
Pd1	$3g$	0.26315(13)	0	$\frac{1}{2}$	1	0.013(1)
M2(Pd)	$3f$	0.60266(17)	0	0	0.633(5)	0.017(1)
M2(Mn)	$3f$	0.60266(17)	0	0	0.367(5)	0.017(1)
Si1	$2d$	$\frac{1}{3}$	$\frac{2}{3}$	$\frac{1}{2}$	1	0.016(1)
Si2	$1a$	0	0	0	1	0.013(1)

Pd-Mn-Ge, $a = 6.7637(14) \text{ \AA}$ , $c = 3.3703(14) \text{ \AA}$ , $R = 3.2\%$						
Atom	Wyckoff Symbol	$x$	$y$	$z$	occupancy	$U_{eq.}(\text{\AA}^2)$
Pd1	$3g$	0.27052(18)	0	$\frac{1}{2}$	1	0.013(1)
M2(Pd)	$3f$	0.6093(2)	0	0	0.823(5)	0.012(1)
M2(Mn)	$3f$	0.6093(2)	0	0	0.177(5)	0.012(1)
Ge1	$2d$	$\frac{1}{3}$	$\frac{2}{3}$	$\frac{1}{2}$	1	0.015(1)
Ge2	$1a$	0	0	0	1	0.013(1)

(No. 25). The calculated composition can be written  $Pd_{1.5}Mn_{0.5}Si$  and is quite proximal to the experimental composition. The electronic structure calculations used linear muffin tin orbitals (LMTO) within the local spin density approximation, as implemented in the STUTTGART TB-LMTO-ASA program.[24, 25] The calculations were performed on 216  $k$  points within the irreducible wedge of the Brillouin zone. The electron localization function (ELF)[26, 27] has been used to understand the extent to which electrons are localized, to locate bonding and non-bonding electron pairs in the real space of the crystal structure.

#### 4. Results and Discussion

Crystallographic details, fractional atomic coordinates and equivalent isotropic displacement parameters are provided for obtained crystal structures in Table 1. The crystal structures of  $PdMnX$  compounds can be viewed as an ordered structure of  $Fe_2P$  with an origin shift of  $00\frac{1}{2}$ , also called the  $ZrNiAl$  type. The compounds crystallize in the noncentrosymmetric hexagonal space group  $P\bar{6}2m$ . The compound  $Pd_{1.63}Mn_{0.37}Si$  is found here to possess the lattice parameters  $a = 6.5033(8) \text{ \AA}$  and  $c = 3.4622(8) \text{ \AA}$ , with a  $c/a$  ratio of 0.53, nearly the same as the values reported for  $Pd_{1.5}Mn_{0.5}Si$  by Bažela,[18] of  $a = 6.4909(6) \text{ \AA}$  and  $c = 3.4655(6) \text{ \AA}$ , also with a  $c/a$  ratio of 0.53. The lattice parameters determined here for  $Pd_{1.82}Mn_{0.18}Ge$  are:  $a = 6.7637(14) \text{ \AA}$ ,  $c = 3.3703(14) \text{ \AA}$ , with a  $c/a$  ratio 0.50. However, in the equiatomic  $PdMnGe$  reported by Vernière *et al.* the  $c/a$  ratio is 0.54.[19]

The structure of  $PdMnX$  is composed of four independent crystallographic sites

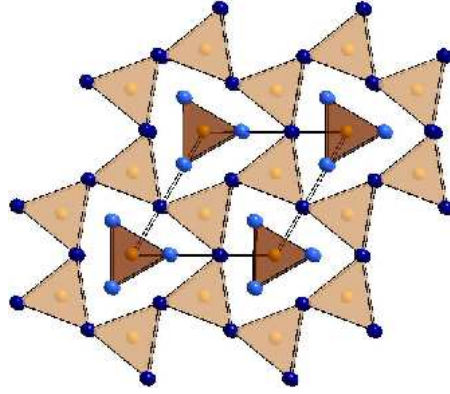


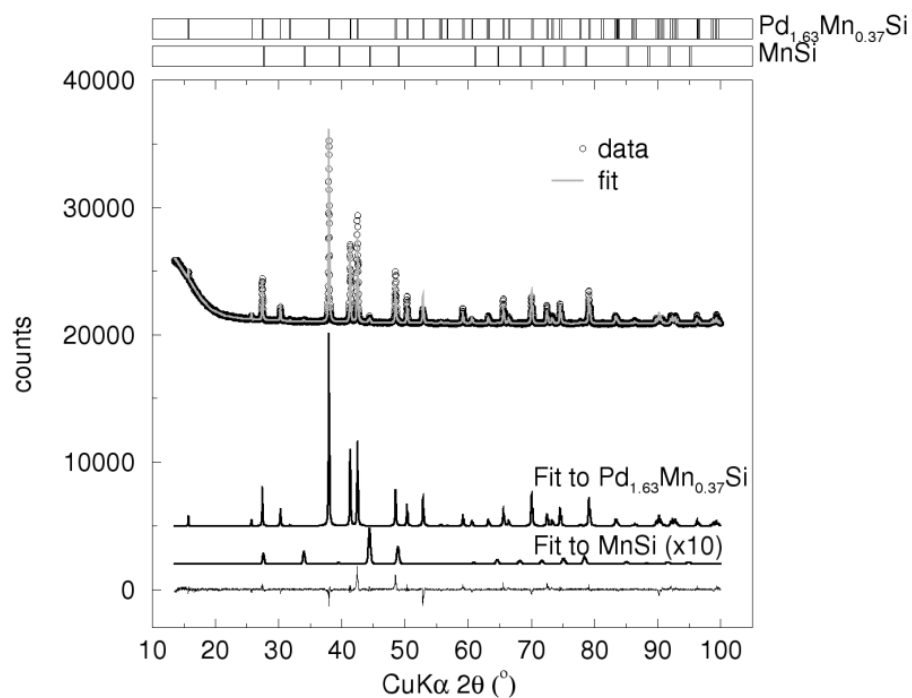
**Figure 1.** Color in online version: Crystal structure of the Pd-Mn-X ( $X = \text{Si}$  or  $\text{Ge}$ ) compounds, showing how X atoms (orange) are in prismatic coordination with the two metal sites: Pd1 are depicted using light blue spheres and the mixed site, M2 is depicted using dark blue spheres. The two kinds of prisms are shifted down the  $z$ -direction by  $\frac{1}{2}$ .

(Table 1). The position M2( $3f$ ) is a mixed site occupied by Pd and Mn. In contrast, the reported equiatomic compound PdMnGe the has the  $3f$  position is completely occupied with Mn. However, there is no PdMnSi compound reported so far. The projection of the  $xy$  plane is shown in figure 1. The structure is built up from X(Si or Ge)-centered tricapped triangular prisms. The prisms are capped by Pd1 and M2. These triangular prisms are condensed *via* common faces and edges.

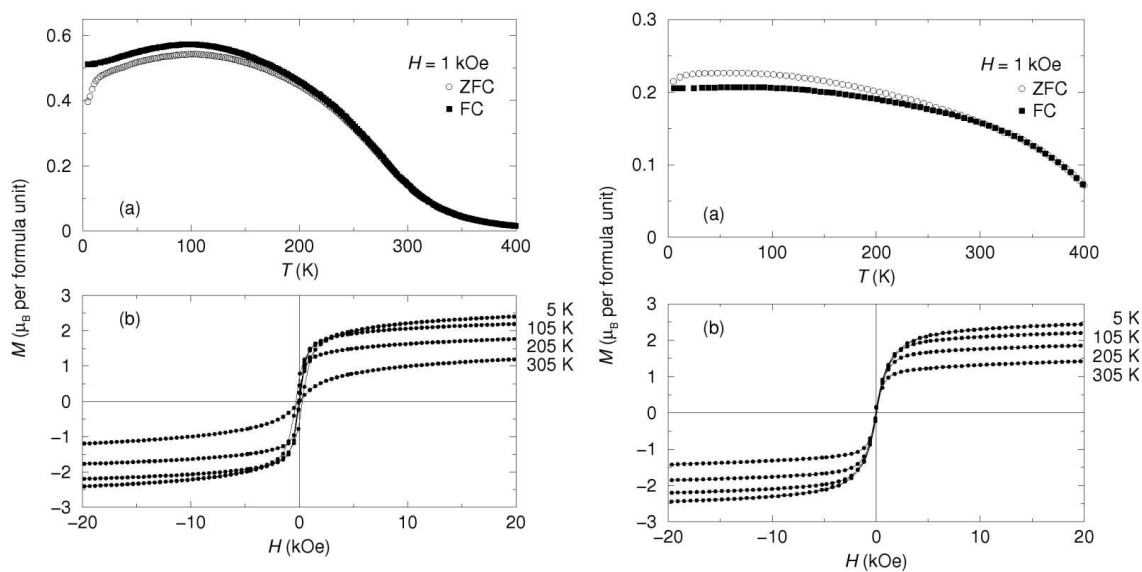
#### 4.1. Pd-Mn-Si

Figure 2 shows Rietveld refinement of the X-ray diffraction profile of  $\text{Pd}_{1.63}\text{Mn}_{0.37}\text{Si}$  using the xND Rietveld code.[28] The starting parameters and site occupancies were taken from single crystal data. The lattice parameters after refinement were  $a = 6.5003(3) \text{ \AA}$  and  $c = 3.4633(2) \text{ \AA}$ , in close agreement with the single crystal data. It is evident from the fit that the sample contains a noticeable amount of MnSi.[29] In addition, the difference profile indicates the possibility of a very small amount of a third phase  $\text{Pd}_2\text{Si}$ , which we have not accounted for in the refinement. The occurrence of these second phases arises from the starting elemental ratios of Pd:Mn:Si of 3:1:2 not matching with the ratio obtained for the single crystal, which is closer to 5:1:3. Johnson and Jeitschko[17] have suggested the possibility of obtaining single phase samples above  $950^\circ\text{C}$ .[17] Our effort to obtain single phase at  $950^\circ\text{C}$  by quenching the sample were not fruitful, and once again, the powder diffractogram revealed the presence of a second MnSi phase.

We have studied the magnetic properties of two different samples in the Pd-Mn-Si system, both whose X-ray diffraction patterns (Rietveld refined lattice parameters) suggest compositions close to that determined by the single-crystal studies, namely  $\text{Pd}_{1.63}\text{Mn}_{0.37}\text{Si}$ . The samples differ in the annealing conditions after arc-melting; samples for which data are displayed in the left and right panels were annealed as reported in the figure caption. Both samples are soft ferromagnets with Curie temperatures above



**Figure 2.** Two-phase Rietveld fit of the Pd-Mn-Si phase. Points are data, and the gray line is Rietveld fit. From top to bottom, the traces are data, fit to  $Pd_{1.63}Mn_{0.37}Si$ , fit to MnSi (magnified 10 times), and the difference profile. Expected peak positions for  $Pd_{1.63}Mn_{0.37}Si$  and MnSi are indicated by the vertical bars at the top of the figure.



**Figure 3.** (a) Zero-field cooled (circles) and field cooled magnetization (filled squares) as a function of temperature, and (b) magnetization as a function of field at four different (indicated) temperatures. The left panels corresponds to a sample of  $Pd_{1.63}Mn_{0.37}Si$  prepared by arc-melting of the elements and then annealed for two days at  $950^\circ$  and 7 days at  $800^\circ C$ , and the right panels of a sample annealed for 5 days at  $800^\circ C$ .

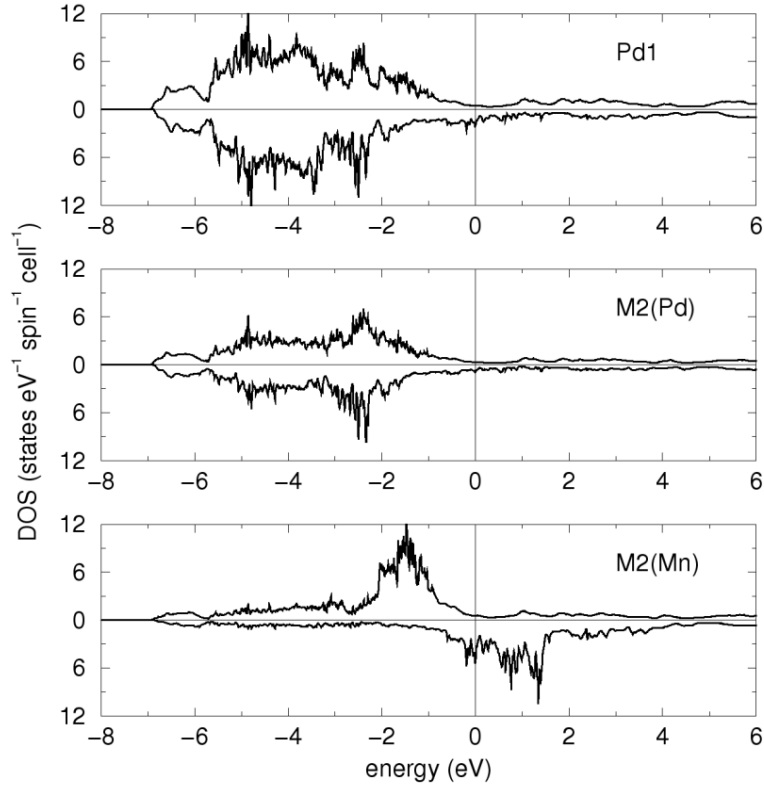


**Figure 4.** Densities of state of  $Pd_5MnSi_3$  showing in three panels, the Pd states from the pure Pd1 site, the Pd states from the mixed M2 site, and the Mn states, also from the mixed M2 site.

the 400 K limit of our SQUID magnetometer. Although the detailed behavior of  $M$  vs.  $T$  for the two samples varies slightly, the nature of the  $M$  vs.  $H$  traces shown in panels (b) are quite similar, with a 5 K saturation magnetization near  $2.4 \mu_B$  per formula unit. The values reported by Bazela[18] for the 3:1:2 composition are  $T_c = 498$  K and the saturation magnetization  $M_{sat}$  of  $2.12 \mu_B$ . This strongly suggests that perhaps the composition in that case as well is closer to what we have observed in the single-crystal analysis. It is important to note that in these samples, the magnetic ion (Mn) is relatively diluted and yet the Curie temperature is quite high. Because of the dilution, it is difficult to associate an integral magnetic moment to the composition, and therefore, it is difficult on the basis of the saturation magnetization alone to determine whether the compound is close to being a half-metal. The powder samples have a small, identifiable MnSi impurity. It is possible that the small downturn in the ZFC trace figure 3, particularly in panel (a) is associated with the magnetic transition of MnSi, which is an itinerant ferromagnet with a  $T_c$  of 29.5 K.[29]

In order to better understand the origin of the magnetism, we have constructed a orthohexagonal supercell of the  $Fe_2P$  structure in the space group  $Pmm2$  (No. 25). LMTO densities of state deriving from the pure and mixed Pd; respectively the Pd1 and M2 sites, and from Mn are displayed separately for the two spin directions in the panels

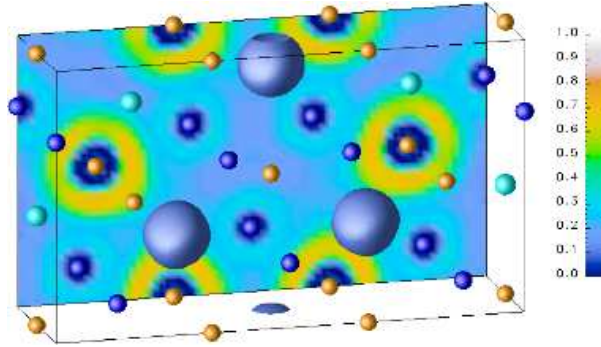


**Figure 5.** Color in online version: Spin density isosurface of  $Pd_5MnSi_3$  for a value of  $0.05 \text{ \AA}^{-3}$  showing that the moment is localized on Mn. The map at the back of the figure displays the valence-only electron localization running from blue (poorly localized) through orange to white (strongly localized).

of figure 4. It is seen that the system is not half metallic since there are both Pd and Mn states in both spin directions. Pd seem to have nearly filled d states, as in common for intermetallic compounds of Pd with early transition elements.[30] The Mn states are strongly spin polarized suggesting local moment behavior in this relatively dilute magnetic compound. This local moment behavior is better visualized by plotting the spin density in the real space of the crystal structure. Figure 5 displays isosurfaces of spin for a value of  $0.05 \text{ \AA}^{-3}$ . It is seen that the spins are well-localized on Mn. In addition, figure 5 shows the valence-only electron localization function plotted as a map of values on the rear plane of the unit cell in the level where Si atoms are found. There is only somewhat spherical localization around the Si and no notable localization on any of the internuclear axes suggesting that this phase cannot be described using notions of local covalent bonding, unlike the half-Heusler compounds.[14] The absence of such covalent bonding can perhaps explain the absence of a half-metallic gap in the title compounds. The calculated magnetic moment per  $Pd_{1.5}Mn_{0.5}Si_2$  is  $1.53 \mu_B$ , somewhat smaller than the experimentally measured value of  $2.2 \mu_B$  for  $Pd_{1.63}Mn_{0.37}Si_2$ . The discrepancy could arise because the DFT calculations are obliged to assume artificial ordering of Mn and Pd.

#### 4.2. Pd-Mn-Ge

When polycrystalline samples in the Pd-Mn-Ge systems were prepared with starting Pd:Mn:Ge ratios of 3:1:2, the orthorhombic  $Pd_3MnGe_2$ [18, 23] phase was formed, always coexisting with a second hexagonal phase. When the starting composition was dictated by the single crystal structural analysis of the hexagonal phase, pure polycrystalline samples were obtained that could be subject to Rietveld analysis of the X-ray powder diffraction patterns. The lattice parameters obtained from the Rietveld analysis were  $a = 6.7701(6) \text{ \AA}$  and  $c = 3.3738(4) \text{ \AA}$  in good agreement with single crystal data. Note that the reported lattice constants for equiatomic hexagonal PdMnGe are  $a = 6.6453(9) \text{ \AA}$  and  $c = 3.36002(5) \text{ \AA}$ , [19], suggesting a homogeneity range.



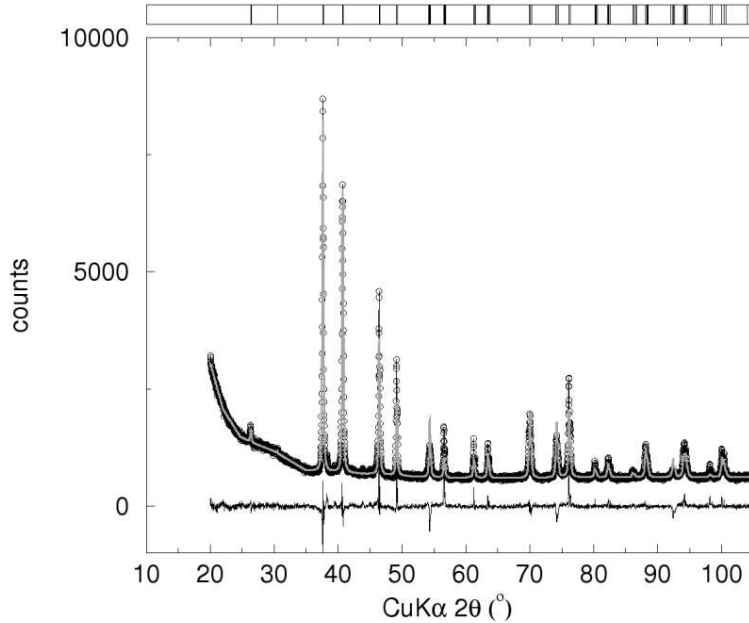


**Figure 6.** Rietveld fit of polycrystalline  $Pd_{1.82}Mn_{0.18}Ge$ . Points are data, and the gray line is Rietveld fit. Below these is the difference profile. Expected peak positions are indicated by the vertical bars at the top of the figure.

Magnetization as a function of temperature and as a function of field for polycrystalline  $Pd_{1.82}Mn_{0.18}Ge$  is shown in figure 7. As a function of temperature under a 1000 Oe field, it is seen that magnetic ordering sets in near 360 K. However,  $M$  vs.  $H$  traces do not show clear evidence for magnetic saturation, unlike the related silicide compounds, suggesting that while the polycrystalline samples seem phase-pure by X-ray diffraction, they may not be magnetically homogeneous. At 5 K and 20 kOe, the observed  $M$  for  $Pd_{1.82}Mn_{0.18}Ge$  is  $0.85 \mu_B$  per formula unit. The values reported for equiatomic  $PdMnGe$  ( $T_c = 541$  K and  $M_{sat} = 3.5 \mu_B$  6 K)[19] are significantly different. However, the values we find are not very different from those determined for  $Pd_3MnGe_2$  ( $T_c = 392$  K and  $M_{sat} = 1.60 \mu_B$ ).[18] If our samples can be considered to be magnetically homogeneous, then it is possible that the lower  $T_c$  and the lower  $M_{sat}$  are related simply to the smaller Mn content.

## 5. Conclusion

Our interest in half-metallic ferromagnets deriving from the equiatomic half-Heusler crystal structure have led us to explore new compounds in the Pd-Mn-Si and Pd-Mn-Ge systems. The compositions and structure of these compounds were established by single crystal methods, and magnetic studies were performed on polycrystalline samples prepared according to compositions dictated by the single crystal structure determination. The sequence of experiments suggests the importance of single crystal structure determinations in exploring new magnetic phases. The title compounds are

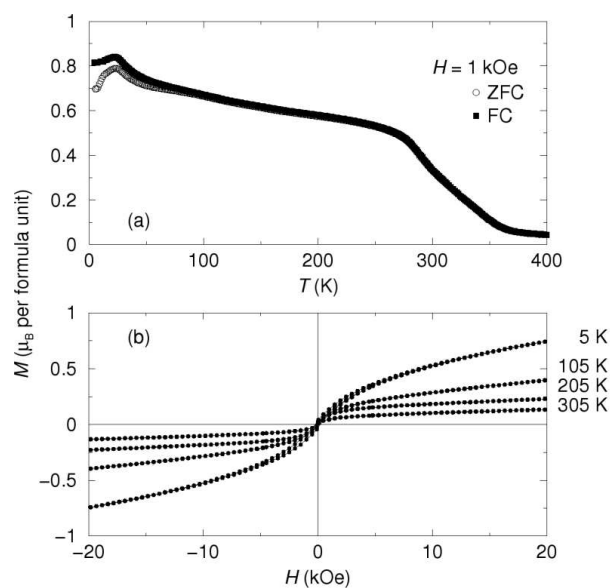


**Figure 7.** (a) Zero-field cooled (circles) and field cooled magnetization (filled squares) as a function of temperature for polycrystalline  $Pd_{1.82}Mn_{0.18}Ge$  compound. (b) Magnetization as a function of field for  $Pd_{1.82}Mn_{0.18}Ge$  at four different (indicated) temperatures.

not half-metallic, perhaps as a result of their not being derived from a covalent network with a tendency to semiconducting behavior. Nevertheless, the silicide compound is interesting because it has a Curie temperature significantly higher than the room temperature despite having a relatively low concentration of magnetic Mn atoms.

## Acknowledgments

ST and RS gratefully acknowledge the National Science Foundation for support through a Career Award (NSF-DMR 0449354) to RS, and for the use of MRSEC facilities (Award NSF-DMR 0520415). We thank Barnaby Dillon for his contribution, and Dr. Guang Wu for help with single crystal data acquisition.

## References

- [1] de Groot R A, Mueller F M, van Engen P G and Buschow K H J 1983 *Phys. Rev. Lett.* **50** 2024
- [2] Hansen K E H M, Mijnders P E 1986 *Phys. Rev. B.* **34** 5009
- [3] Hansen K E H M, Mijnders P E, Rabou L P L M, Buschow K H J, 1990 *Phys. Rev. B.* **42** 1533
- [4] Zhu W, Sinkovic B, Vescovo E, Tanaka C, Moodera J S 2001 *Phys. Rev. B.* **64** 060403
- [5] Correa J S, Eibl Ch, Rangelov G, Braun J, Donath M 2006 *Phys. Rev. B.* **73** 125316
- [6] Jarrett H S, Cloud W H, Bouchard R J, Butler S R, Frederick C G and Gillson J L 1968 *Phys. Rev. Lett.* **21** 617
- [7] Horikawa J I, Hamajima T, Ogata F, Kambara T and Gondaira K I 1982 *J. Phys. C: Solid State Phys.* **15** 2613
- [8] Jonker G H and van Santen J H 1950 *Physica* **16** 337
- [9] Žutić I, Fabian J and Das Sarma S 2004 *Rev. Mod. Phys.* **76** 323

- [10] Felser C, Fecher G and Balke B 2007 *Angew. Chem. Intl. Edn. Engl.* **46** 668
- [11] Jung D, Koo H-J and Whangbo M-H 2000 *J. Mol. Struct. Theochem.* **527** 113
- [12] Ögüt, S and Rabe K M 1995 *Phys. Rev. B* **51** 10443
- [13] Galanakis I, Mavropoulos Ph and Dederichs P H 2006 *J. Phys. D: Appl. Phys.* **39** 765
- [14] Kandpal H C, Felser C and Seshadri R 2006 *J. Phys. D: Appl. Phys.* **39** 776
- [15] Kübler J, Williams A R and Sommers C B 1983 *Phys. Rev. B* **28** 1745
- [16] Galanakis I, Dederichs P H and Papanikolaou N 2002 *Phys. Rev. B* **66** 174429
- [17] Johnson V and Jeitschko W 1972 *J. Solid State Chem.* **4** 123
- [18] Bažela W 1984 *J. Less-common Met.* **100** 341
- [19] Vernière A, Tobola J, Venturini G and Malaman B 1999 *J. Magn. Magn. Mater.* **207** 95
- [20] Ericksson T, Mellergård A, Nordblad P, Larsson, A-K, Felton S, Höwing J, Gustafsson T and Andersson Y 2005 *J. Alloys Compounds* **403** 19
- [21] SADABS program for absorption correction, G.M. Sheldrick for Bruker Analytical X-ray Instrument Inc. Madison, WI 1997
- [22] SMART and SAINT, Data collection and processing software for the SMART system, Bruker Analytical X-ray Instrument Inc. Madison, WI 1997
- [23] Venturini G, Malaman B, Steinmetz J, Courtois A and Roques B 1982 *Mat. Res. Bull.* **17** 259
- [24] Andersen O K 1975 *Phys. Rev. B* **12** 3060
- [25] Jepsen O and Andersen O K 2000 STUTTGART TB-LMTO-ASA Program version 47, MPI für Festkörperforschung, Stuttgart, Germany
- [26] Becke A D and Edgecombe K E 1990 *J. Chem. Phys.* **92** 5397
- [27] Silvi B and Savin A 1994 *Nature* **371** 683
- [28] Bézar J F and Garnier P 1992 Computer code XND available from the Web site at <http://www.ccp14.ac.uk>
- [29] Pfleiderer C, Reznik D, Pintschovius L, Löhneysen H v, Garst M and Rosch A 2004 *Nature* **427** 227
- [30] Brewer L and Wengert P R 1973 *Metall. Trans.* **4** 83